Fifth International Conference on CFD in the Process Industries
CSIRO, Melbourne, Australia
13-15 December 2006

COMPUTATIONAL SIMULATION OF RED BLOOD CELL DEFORMATION AND RADIAL MIGRATION IN MICROVESSELS

Timothy W. SECOMB[1], Beata STYP-REKOWSKA[2] and Axel R. PRIES[2,3]

[1] Department of Physiology, University of Arizona, Tucson, AZ 85724, USA

[2] Charité - Universitätsmedizin Berlin, Campus Benjamin Franklin, Dept. of Physiology, Arnimallee 22, 14195 Berlin, Germany

[3] Deutsches Herzzentrum Berlin, Augustenburger Platz 1, D-13353 Berlin, Germany

ABSTRACT

The motion and deformation of mammalian red blood cells (RBCs) in microvessels are simulated using a two-dimensional computational model. Each RBC is represented as a set of interconnected viscoelastic elements suspended in a viscous fluid. The equations of equilibrium of this structure are solved simultaneously with the equations of fluid motion using a finite-element method. Computed cell shapes ane trajectories are compared with corresponding experimental observations and good agreement is shown. The method is used to predict the motion of multiple interacting RBCs flowing along narrow tubes.

INTRODUCTION

Human blood contains 40-45% by volume of red blood cells (RBCs), which exert a strong influence on the flow properties of blood. Mechanically, a RBC may be considered as a highly flexible membrane containing an incompressible viscous fluid. In the microcirculation, the cells dimensions (~8 μm undeformed diameter) is comparable to microvessel dimensions (4-100 μm).

Several theoretical approaches have been developed to describe motion of RBCs in microvessels. Quantitative theoretical models have been developed that successfully predict flow resistance when RBCs flow in single file in narrow capillary-sized tubes (Secomb et al. 1986). In tubes with diameter about 30 μm or more, flow resistance can be predicted using a two-phase continuum model, in which a central core region with uniform viscosity is surrounded by a cell-free layer having an empirically determined width of 1.8 μm (Secomb 1995; Secomb 2003). However, no quantitative theory is available to predict the width of the cell-free layer from first principles based on the mechanical properties of RBCs.

Simulation of the motion of multiple interacting flexible particles in three dimensions is a difficult computational problem. In the present study, a two-dimensional model is therefore used. However, the mechanical properties of the particles representing RBCs are chosen to simulate key aspects of their three-dimensional mechanics.

MODEL DESCRIPTION

The two-dimensional representation of RBC mechanics is shown in Figure 1A. The membrane lying in a cross-section through a three-dimensional cell is a represented as a chain of straight elements, hinged at the nodal points. Each element consists of an elastic component in parallel with a viscous component, representing the viscoelastic properties of the membrane. An elastic resistance to bending is introduced at the nodes, to represent membrane bending elasticity.

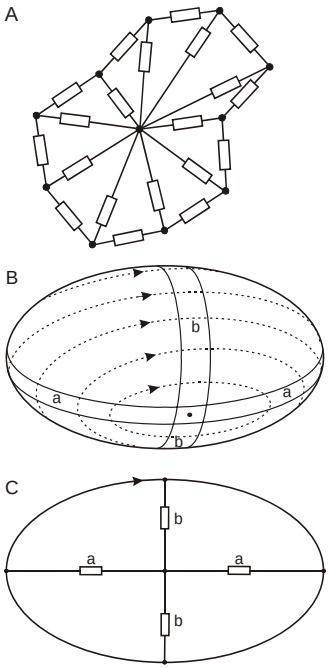

Figure 1. A. Two-dimensional model for RBC. Rectangles represent viscoelastic elements. B, C. Relationship between internal viscous elements and membrane deformation in tank-treading. Bands of membrane (a,b) alternately shorten and elongate during tank-treading.

When placed in simple shear flow of high-viscosity fluid, RBCs exhibit stable orientations and cyclic 'tank-treading' motion of the membrane around the cell interior. In this motion, a band of membrane around the cell is alternately lengthened and shortened (Figure 1B). This continuous deformation results in viscous energy dissipation in the membrane. Internal viscous elements connecting each nodal point to a single central point within the model cell are included to represent resistance to this motion.

The fluid flow around the model cell results in loadings on the external elements. The longitudinal (tension) force $t_i(s)$, the transverse (shear) force $q_i(s)$ and the bending

moment $m_i(s)$ acting in external element i are consequently functions of distance s along the element from node i to node i+1, where $0 \le s \le l_i$ and l_i is the length of the element, and where $1 \le i \le n$ and n is the number of external nodes and elements. The equations of mechanical equilibrium for an element are

$$dt_i/ds = -g_i \quad (1)$$

$$dq_i/ds = -f_i \quad (2)$$

$$dm_i/ds = q_i \quad (3)$$

where $f_i(s)$ and $g_i(s)$ are the normal and tangential components of the fluid loading. The viscoelastic behaviour of the external segments is represented by

$$\bar{t}_i = k_t(l_i/l_0 - 1) + \mu_m \frac{1}{l_i}\frac{dl_i}{dt} \quad (4)$$

where $\bar{t}_i$ is the mean tension in external element i, l_0 is the reference length of the element, k_t is the elastic modulus and μ_m is the viscosity. The bending moments acting on element i at nodes i and i +1 are given by

$$m_i(0) = -k_b\alpha_i/l_0$$

$$m_i(l_i) = -k_b\alpha_{i+1}/l_0 \quad (5)$$

where k_b is the bending modulus and $\alpha_i = \theta_i - \theta_{i-1}$ is the angle between elements $i - 1$ and i. Integrating equation (3) gives

$$\bar{q}_i = k_b(\alpha_i - \alpha_{i+1})/(l_0\, l_i)\,. \quad (6)$$

where $\bar{q}_i$ is the mean transverse force in external element i. From these equations, the tensions and transverse forces at the end points of each element can be obtained. The internal elements are assumed to be viscous:

$$T_i = \mu'_m \frac{1}{L_i}\frac{dL_i}{dt} \quad (7)$$

where L_i is the length of internal element i and μ'_m is its viscosity. For any given configuration of the cell, the conditions for overall equilibrium of forces acting at the external nodes and the central node can then be expressed as a linear system involving the fluid loads $f_i(s)$ and $g_i(s)$ on each external segment and the velocities of the nodes.

RBCs deform at effectively constant volume. This property is represented by assigning an internal pressure that depends on the cell area A:

$$p_{int} = k_p(1 - A/A_{ref}) \quad (8)$$

where A_{ref} and k_p are constants. A large value of k_p is used (e.g., 50), so that the cell strongly resists area changes and the area remains close to the reference value A_{ref}.

The suspending medium is a viscous incompressible fluid, and the components of stress in the fluid are

$$\sigma_{xx} = 2\mu\,\partial u/\partial x - p,$$

$$\sigma_{xy} = \mu\,(\partial v/\partial x + \partial u/\partial y)$$

$$\sigma_{yy} = 2\mu\,\partial v/\partial y - p \quad (9)$$

where $p(x,y)$ and $(u(x,y),\ v(x,y))$ are the pressure and velocity fields. Inertia is negligible, and conservation of momentum implies that

$$\partial\sigma_{xx}/\partial x + \partial\sigma_{xy}/\partial y = 0$$

$$\partial\sigma_{xy}/\partial x + \partial\sigma_{xy}/\partial y = 0. \quad (10)$$

The divergence of the flow is $e = \partial u/\partial x + \partial v/\partial y$, where $e = 0$ in an incompressible fluid. The velocity at each point on an external element is obtained by linear interpolation between the nodal velocities at its ends and must match the local fluid velocity according to the no-slip condition.

A finite element package (FlexPDE version 3.11, PDE Solutions Inc., Antioch, CA) was used to solve the resulting system of coupled equations. The incompressibility condition $e = 0$ cannot be specified as one of the governing equations because of the structure of FlexPDE. The condition $e = 0$ can be satisfied approximately by setting $\nabla^2 p = Ke$ where K is a large constant (e.g., 100), and monitoring values of e. The components (u_i, v_i) of velocity at node i and at the central node were introduced into the finite element formulation as scalar variables. RBC shapes were generally represented using 20 nodes, and 100-400 fluid elements were typically used. When a cell closely approaches the domain boundary or another cell, the mesh generator controls the aspect ratio of the elements, so that a large number of small elements are used, allowing resolution of steep pressure and velocity gradients.

Time-dependent cell shapes were computed using an explicit (Euler) scheme, with a time step of 1 ms or less. Smaller time steps were used for calculations of cell motions in shear flow at high shear rates and viscosities. Each time step required approximately 100s on a personal computer with a 2 GHz processor. The initial shape was assumed to be circular with area A_{ref}, so as not to bias the subsequent evolution of cell shape. As the motion proceeds, the external segments elongate from initially compressed states, allowing non-circular shapes with the same area.

Scaled values of variables were used. All distances were expressed in μm, times in ms and forces in units of 10^{-7} dyn. The corresponding unit of viscosity is then 1 cP, close to the viscosity of normal blood plasma. The dimensionless elastic constants of the membrane are then 0.18 for bending modulus, 6 for shear modulus, and 5×10^5 for bulk modulus. From these values, it is evident that elastic bending resistance is generally a small effect, shear resistance is significant and resistance to area change is very high. The scaled shear viscosity of the membrane is 1000. Therefore, the cell has a large viscous resistance to deformation on the millisecond timescale. In the two-dimensional model, values of these parameters and the viscosity of the internal elements were adjusted to provide a close fit to experimentally observed behaviour of RBCs tank-treading in high-viscosity media, including variation of cell length and tank-treading frequency with shear rate. Further simulations were then performed using channel geometries representative of red cell motion in microvessels, including effects of asymmetric cell position.

RESULTS

Predictions for a single cell flowing along an 8-μm channel are compared in Figure 2 with experimental observations in glass tubes. Good qualitative agreement with observed shapes is seen. Results are shown in Figure 3 for a RBC in a bifurcation observed in the rat mesentery. Motions of several cells surrounded by plasma, without any closely interacting cells, were observed in successive video frames and digitized. The vessel outline was also digitized and used to define the domain for corresponding simulations. Close agreement between observed and

predicted centre-of-mass trajectories was obtained (results not shown). Trajectories of cells with different starting points relative to the vessel walls were found to converge after a distance of about 60 μm.

To simulate the motion of multiple interacting RBCs, periodic boundary conditions were used to represent a repeating configuration of cells. As illustrated in Figure 4, RBCs underwent large deformations and close mechanical interactions in the simulated flow. They also showed a tendency to migrate away from the wall, which was counteracted by cell-cell interactions. Further investigation of this phenomenon is needed to understand the factors determining the width of the cell-free layer.

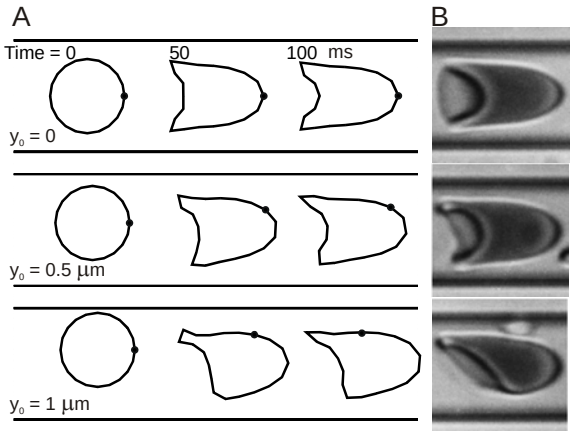

Figure 2. Predicted motion and deformation of cells flowing in an 8-μm channel. Flow rate is adjusted so that cell velocity is approximately 1.25 mm/s. Results are presented for cells with initial displacements 0, 0.5, 1 μm from the centre-line. A. Predicted cell shapes initially and after 50 and 100 ms. Dot on cell outline represents a node fixed in the cell. B. Observed human RBC shapes in a single glass capillary with diameter 7 μm. Three cells are shown with varying orientations and degrees of asymmetry.

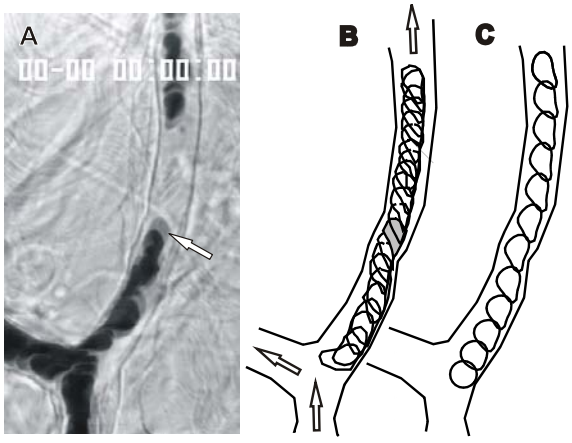

Figure 3. Observations and simulations of RBC motion in rat mesenteric microvessels. A. Microvessels selected for observation. Arrow: RBC whose motion was tracked. B. Superimposed digitized outlines of vessel wall and of selected isolated cells in successive video frames at 10-ms intervals. Arrows show flow directions. C. Predicted cell shapes at 20-ms intervals.

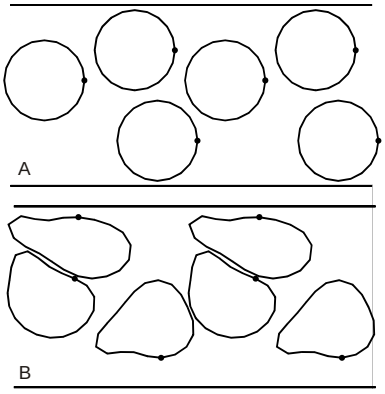

Figure 4. Simulated motion of three interacting cells in a 12-μm channel, using periodic boundary conditions. A. Initial configuration. B. After 50 ms.

CONCLUSION

This two-dimensional method predicts shapes and trajectories of individual RBCs flowing in capillaries in good agreement with observations, and provides a method for simulating the motion of multiple interacting RBCs.

Supported by NIH Grant HL034555.

REFERENCES

SECOMB, T.W., (1995). "Mechanics of blood flow in the microcirculation." S*ymp. Soc. Exp. Biol.*, **49**, 305-321.

SECOMB, T.W., (2003). "Mechanics of red blood cells and blood flow in narrow tubes." *Hydrodynamics of Capsules and Cells*, C. Pozrikidis, ed., Chapman & Hall/CRC, Boca Raton, Florida, 163-196.

SECOMB, T.W., SKALAK, R., OZKAYA, N., and GROSS, J.F., (1986). "Flow of axisymmetric red blood cells in narrow capillaries." *Journal of Fluid Mechanics*, **163**, 405-423.